Comparison of Near Real-Time DMSP SSM/I Daily Polar Gridded Products and SSM/I Polar Gridded Products

J. Stroeve and J. Smith

May 2001

National Snow and Ice Data Center (NSIDC) Special Publication 10

Introduction

The National Snow and Ice Data Center (NSIDC) archives and distributes polar stereographic gridded brightness temperature and sea ice concentration products derived from passive microwave satellite data. Currently, NSIDC produces two different sets of brightness temperature and sea ice concentration products using data from the Defense Meteorological Satellite Programs Special Sensor Microwave/Imager (DMSP SSM/I). The DMSP SSM/I Daily Polar Gridded Brightness Temperatures product is referred to as the *standard brightness temperature product*. The DMSP SSM/I Daily and Monthly Polar Gridded Sea Ice Concentrations product is derived from the brightness temperatures and is referred to as the *standard sea ice product*. The standard brightness temperature product is created using raw DMSP antenna temperatures that are processed by Remote Sensing Systems, Inc. (RSS). Because RSS performs various calibration and geolocation checks on the initial raw satellite data, there is a time lag of approximately three to six months after the date of acquisition before NSIDC receives the antenna temperatures from RSS and data are distributed to users. The standard product data are available for dates beginning 9 July 1987. Processing is ongoing.

Many users, however, need the data before the standard products become available. To facilitate time-sensitive research, NSIDC implemented a Near Real-Time Sea Ice (NRTSI) project. The NRTSI products refer to the Near Real-Time DMSP SSM/I Daily Polar Gridded Brightness Temperatures and the Near Real-Time DMSP SSM/I Daily Polar Gridded Sea Ice Concentrations. The NRTSI project creates identical products as the standard product, but uses data from the Global Hydrological Research Center (GHRC) rather than RSS. These data are available the day after they are collected and are not quality-controlled before they are initially used. However, after a few days GHRC does perform some limited quality control on the brightness temperature data. Since NSIDC repeats its

processing every five days, products that are approximately three days old use the quality-controlled brightness temperatures. For data files less than three days old, the gridded data are most likely produced from data that were not quality-controlled at GHRC. The near-real time data do not supplant the standard products, but instead fill the time gap between present-day and the delivery of the RSS data. Therefore, the NRTSI data are only available until the standard products are released.

This document quantifies possible differences between the standard and near-real time products using the GHRC quality-controlled products for the intercomparison, and will show that GHRC's quality control has little impact on the data.

Methodology

The transformation of raw brightness temperatures into gridded brightness temperature and sea ice concentration products is essentially the same for the two product sets; however, there are some differences. For NRTSI data, NSIDC receives brightness temperatures as swaths of satellite data geolocated at the earth position of each sample. For the standard products the data are similarly received; however, the raw data are antenna temperatures, not brightness temperatures. RSS provides software for calculating brightness temperatures from antenna temperatures. The brightness temperatures are interpolated to the appropriate grids using a drop-in-the-bucket algorithm (Knowles 1993). Sea ice concentrations are then computed from the 19V GHz and 19H GHz brightness temperatures and the 37V GHz brightness temperatures using the NASA Team algorithm (Cavalieri 1996). A weather filter using the 22V GHz channel is also applied.

GHRC Data

GHRC receives SSM/I antenna temperatures from the Fleet Numerical Meteorology and Oceanography Center (FNMOC). GHRC performs two quality control steps before converting the antenna temperatures into brightness temperatures: (1) it corrects for the feedhorn partially seeing the cold-space reflector during the last few samples of each scan (referred to as an along-scan adjustment in the Wentz documentation), and (2) it adjusts for the mean difference between the SSM/I antenna temperatures and the Wentz radiative transfer model-derived antenna temperatures for the ocean and intervening atmosphere. An along-scan adjustment is applied to all channels except 85 GHz. For a more complete description of how GHRC processes SSM/I data, see the GHRC documentation.

NSIDC receives brightness temperatures from GHRC as HDF format files via an ftp link. Each file contains one "pass", defined as a pole-to-pole swath. The

brightness temperature data are converted to NSIDC's "generic swath" format by a program named '*hdftogs*'. A standard interpolation program ('*gsgrid*') reads the generic swath-formatted data and interpolates the brightness temperatures to polar stereographic grids. A final program named '*pmalgos*' computes the sea ice concentration grids.

RSS Data

NSIDC receives antenna temperature data from RSS on 8 mm tapes, in three-month increments. The tapes typically include 24 files, each of which contains data for three or four days. Software to convert the raw antenna temperatures to brightness temperatures accompanies the data. The software also includes various processing options, such as correcting for the cold-space reflector problem. NSIDC used this option for the DMSP F8 data (9 July 1987 through 18 December 1991) and for products generated beyond 1 January 2000. For an analysis of the effect of the along-scan correction, see Stroeve, 1998. Note, however, that RSS does not provide along-scan corrections for the 85 GHz channels.

NSIDC does not use the correction for the difference between the SSM/I antenna temperature observations and the Wentz radiative transfer model-derived antenna temperatures for the ocean and intervening atmosphere, as these corrections may degrade the accuracy of the brightness temperatures over land and sea ice (Wentz 1992). Additionally, RSS developed its own algorithm for geolocating DMSP satellite scans. The differences in scan locations are significantly different from those in the GHRC data, as will be discussed below.

The files on the 8 mm tapes are in a format developed by RSS. The data are first converted to NSIDC's generic swath format by a program that incorporates software supplied by RSS. An additional program, '*gsconcat*', separates the data from the three to four day RSS grouping into files for individual days. Finally, the programs '*gsgrid*' and '*pmalgos*' interpolate the brightness temperatures to polar stereographic grids and produce the sea ice concentration grids, respectively.

Results

To quantify the differences between the NRTSI products and the standard products, a winter and summer month (January and June 2000) are used for comparison. The standard products used in the comparison contain the along-scan adjustment for F13 provided by RSS.

Brightness Temperature Comparison

Brightness temperature grids for each channel from both products are compared for the entire month. The absolute value of the daily differences at each grid cell are computed, and results are binned into seven categories:

- number of grid cells that have the same value
- number of grid cells differing by .1K
- number of grid cells differing by between .2 and .4K
- number of grid cells differing by between .5 and 1K
- number of grid cells differing by between 1.1 and 2K
- number of grid cells differing by between 2.1 and 3K
- number of grid cells differing by more than 3K

Figures 1-4 show the monthly percentage of grid cells that fall in each bin. There is a separate bar graph for each channel and hemisphere. The graphs show that differences between the corresponding products can be large. In all cases, the percentage of grid cells where the brightness temperature differs by more than 2K exceeds the percentage where the brightness temperatures are equal. The percentage of grid cells with significant differences is greater for horizontally-polarized than for vertically-polarized channels; and greater for the 85GHz channels than for the lower frequency channels.

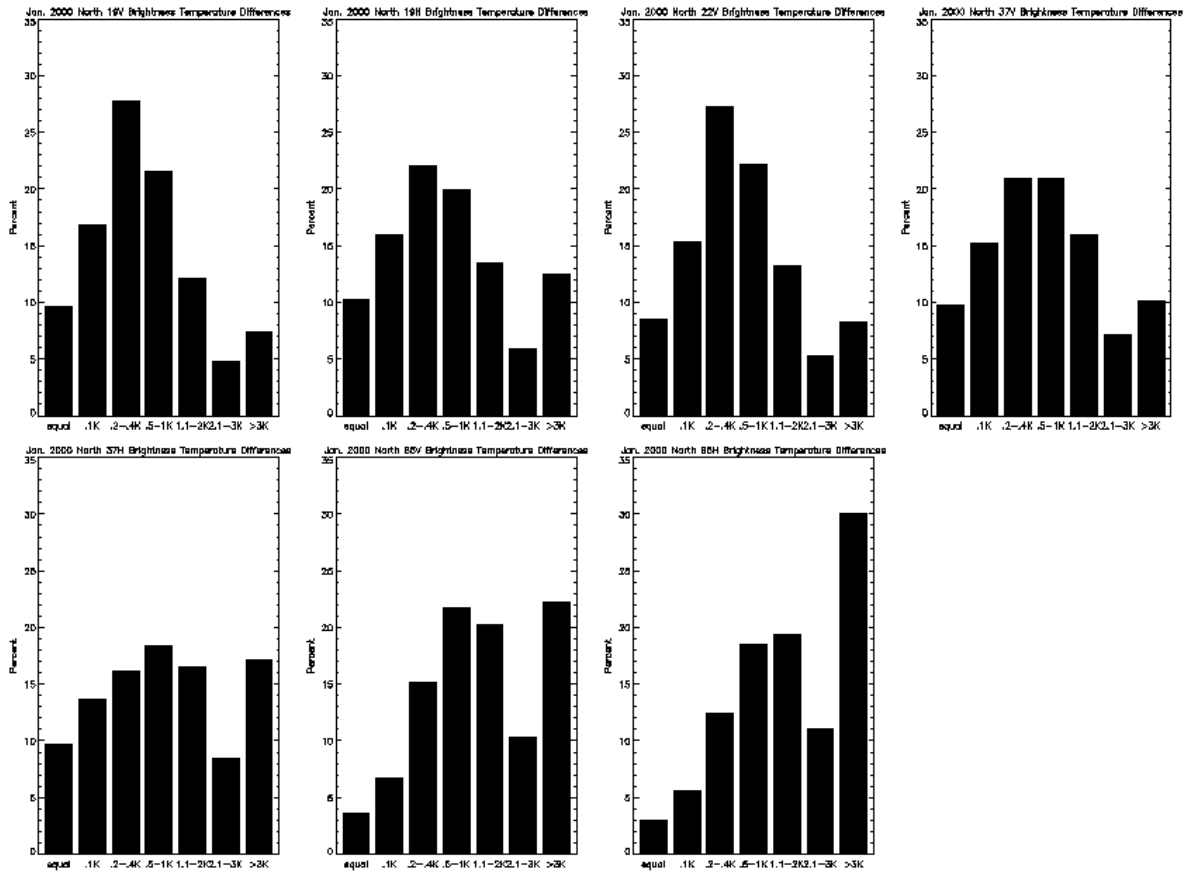

Figure 1. January 2000 Northern Hemisphere Brightness Temperature Difference Bar Graphs

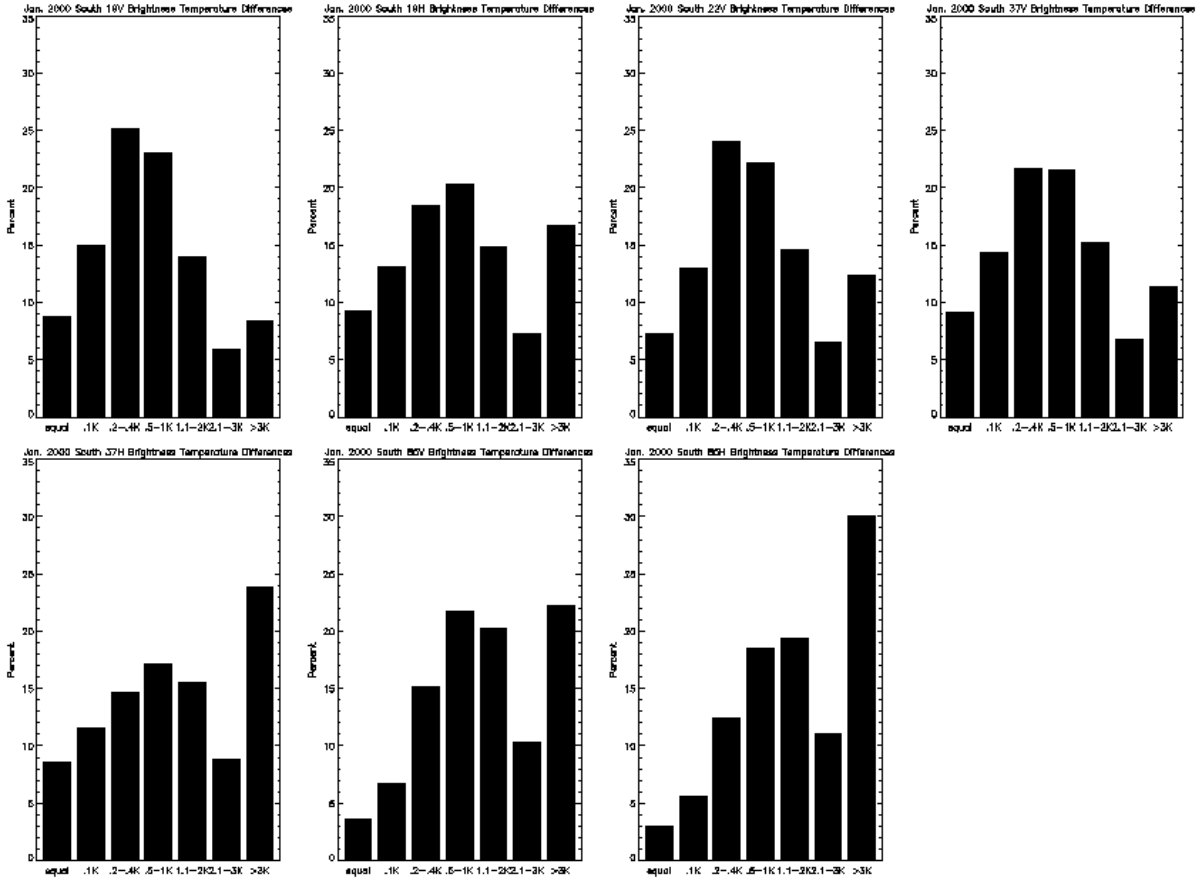

Figure 2. January 2000 Southern Hemisphere Brightness Temperature Difference Bar Graphs

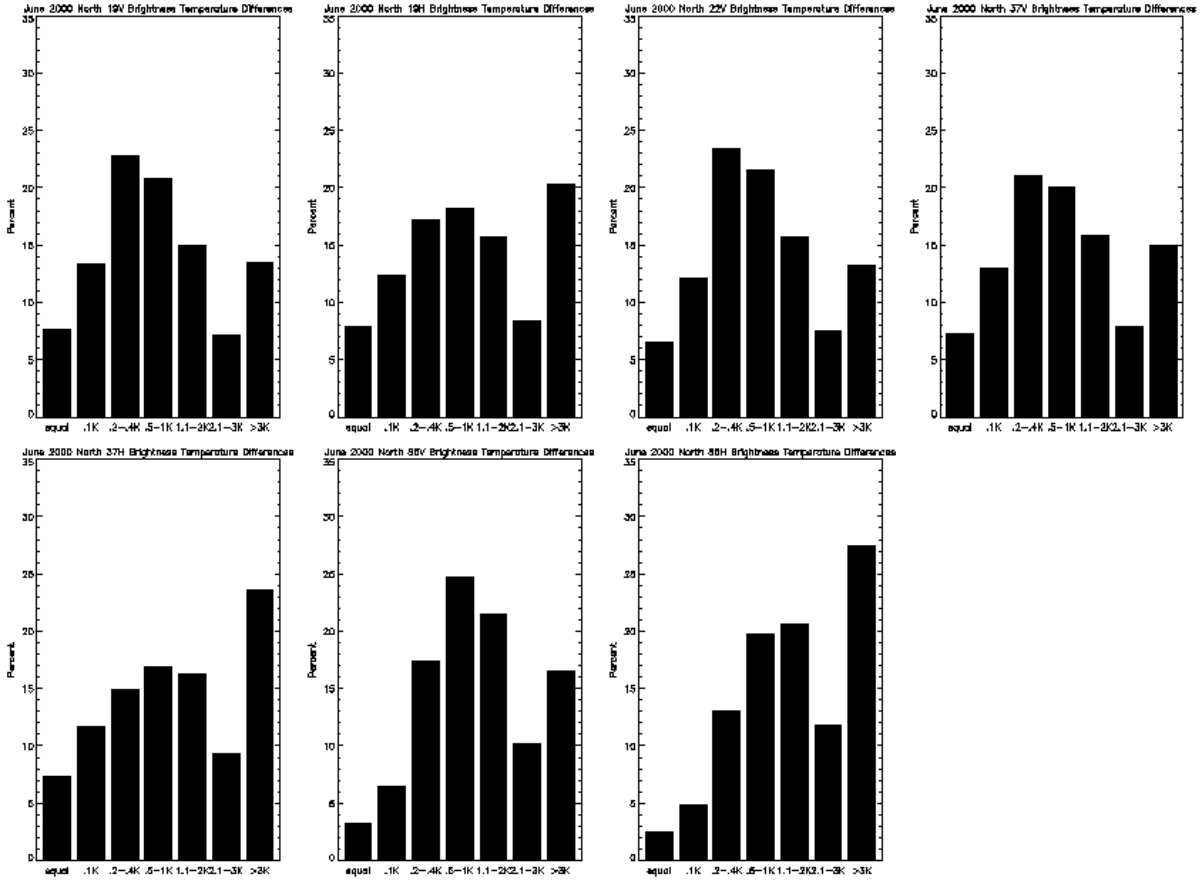

Figure 3. June 2000 Northern Hemisphere Brightness Temperature Difference Bar Graphs

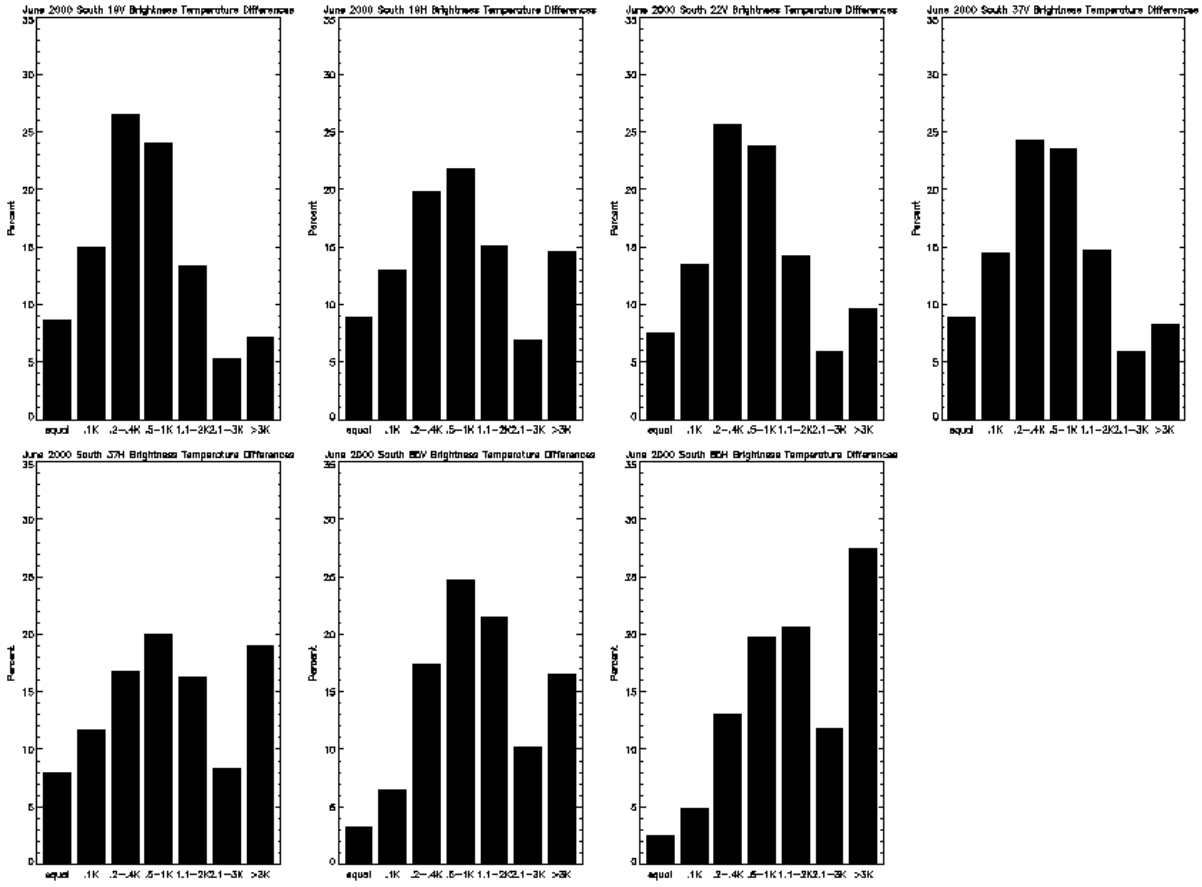

Figure 4. June 2000 Southern Hemisphere Brightness Temperature Difference Bar Graphs

Figures 5-8 show the mean difference in 19 GHz and 37 GHz gridded brightness temperatures at each grid cell for January and June 2000. These differences represent the mean of the absolute differences for each month. The mean differences are greatest along coastlines, sea ice boundaries, and over the open ocean. The smallest differences between the standard products and the NRTSI brightness temperatures occur over sea ice and ice sheets where the brightness temperature gradient is small.

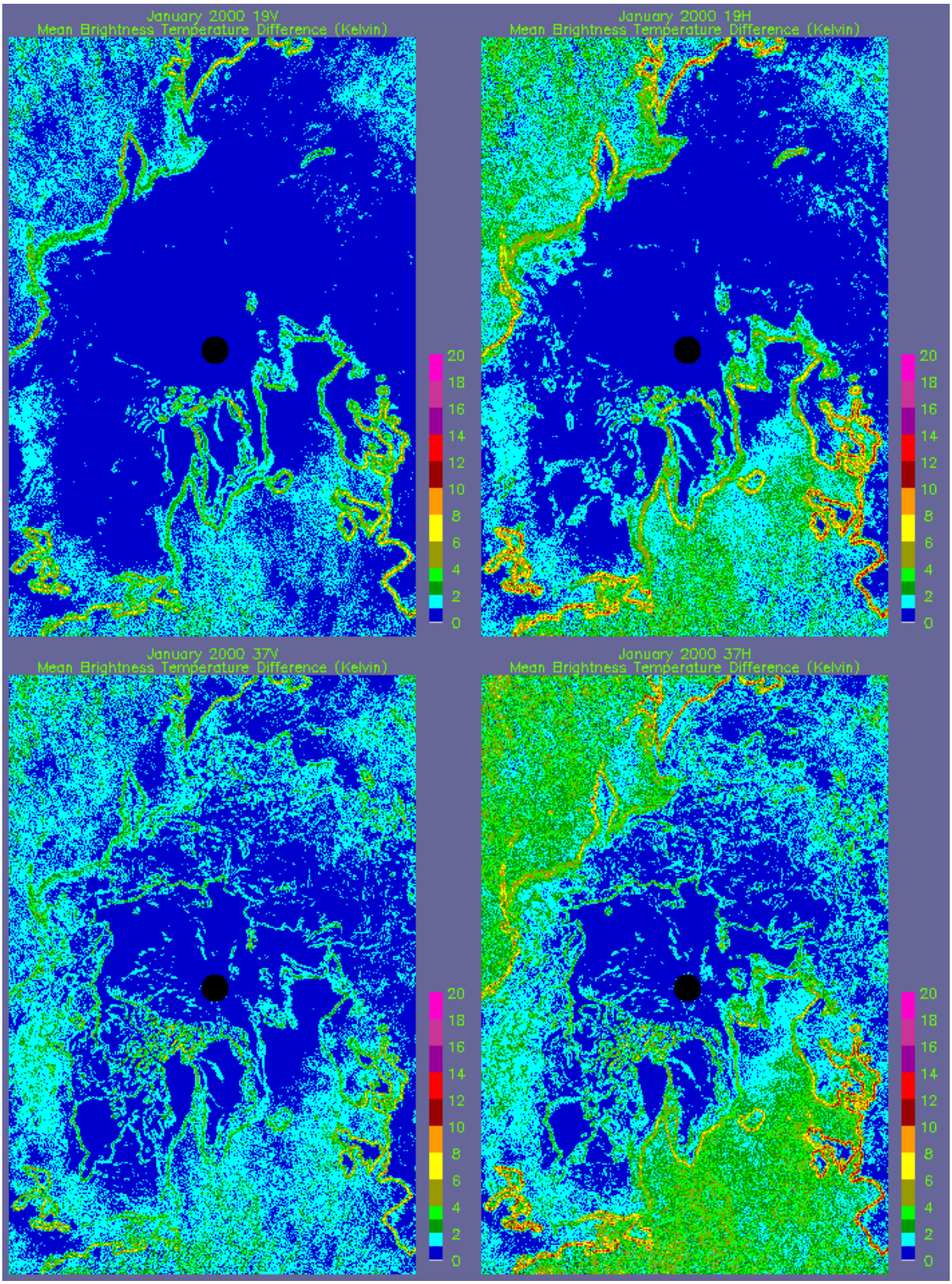

Figure 5. January 2000 Northern Hemisphere Tb Differences

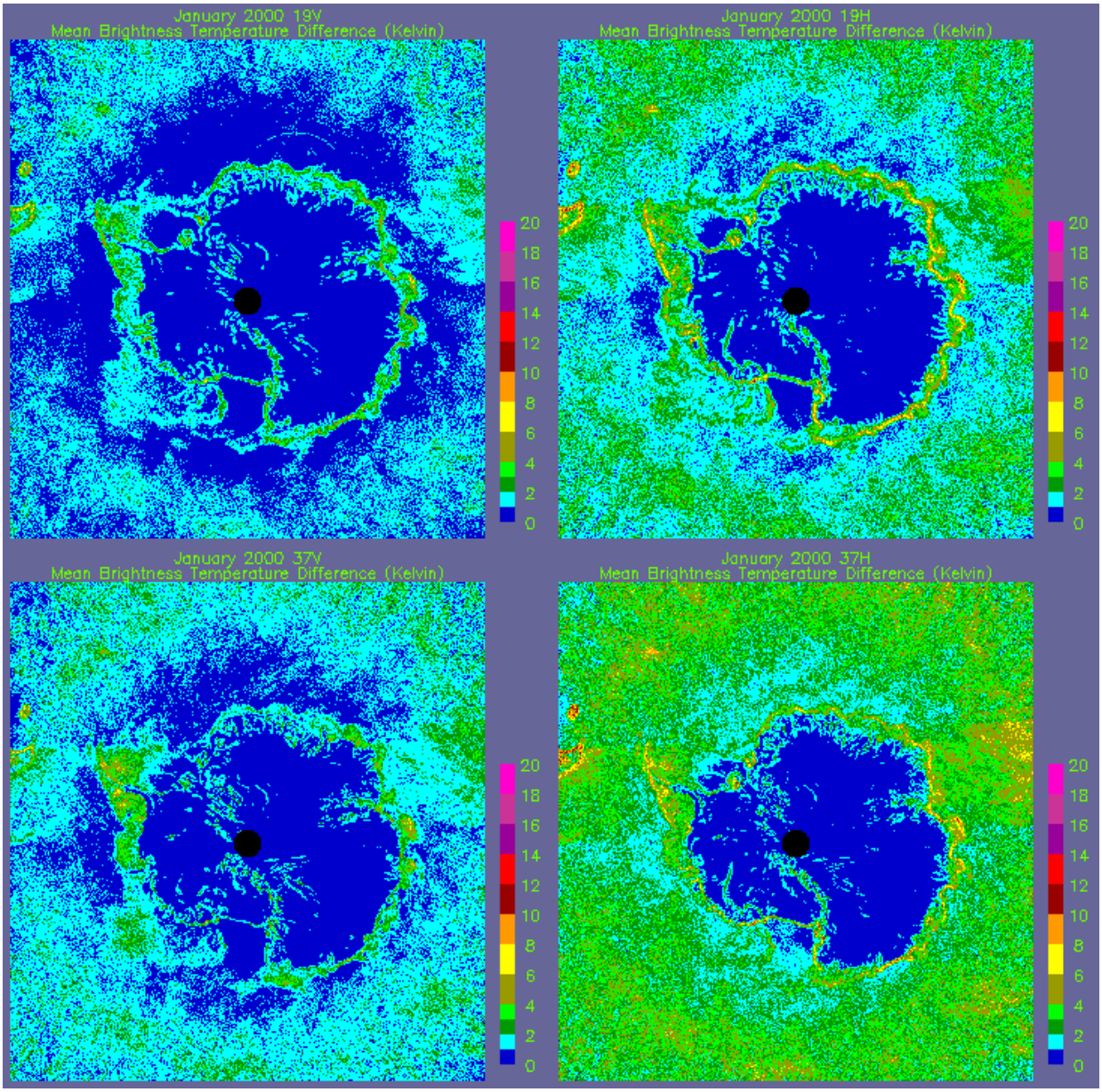

Figure 6. January 2000 Southern Hemisphere Tb Differences

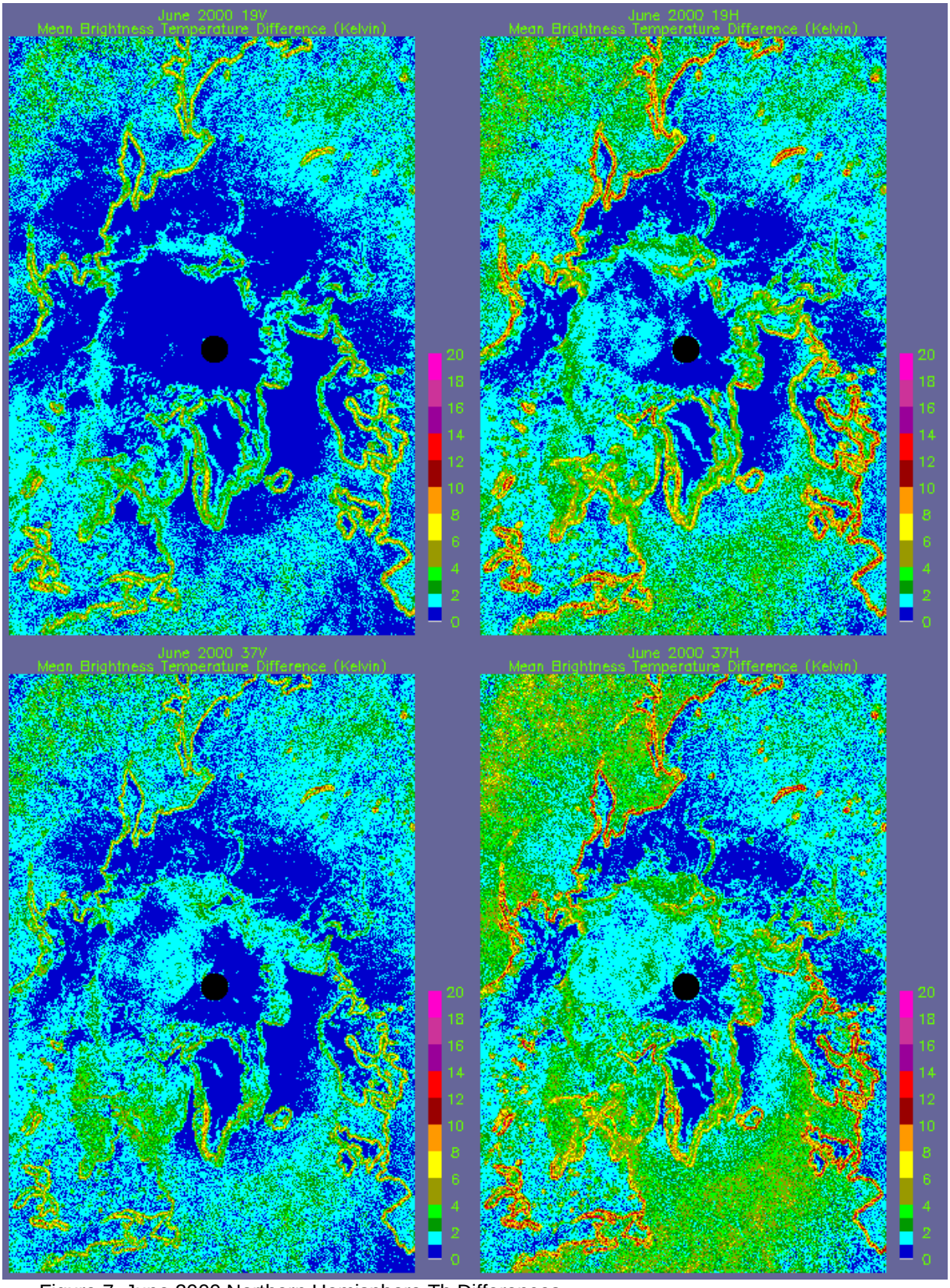

Figure 7. June 2000 Northern Hemisphere Tb Differences

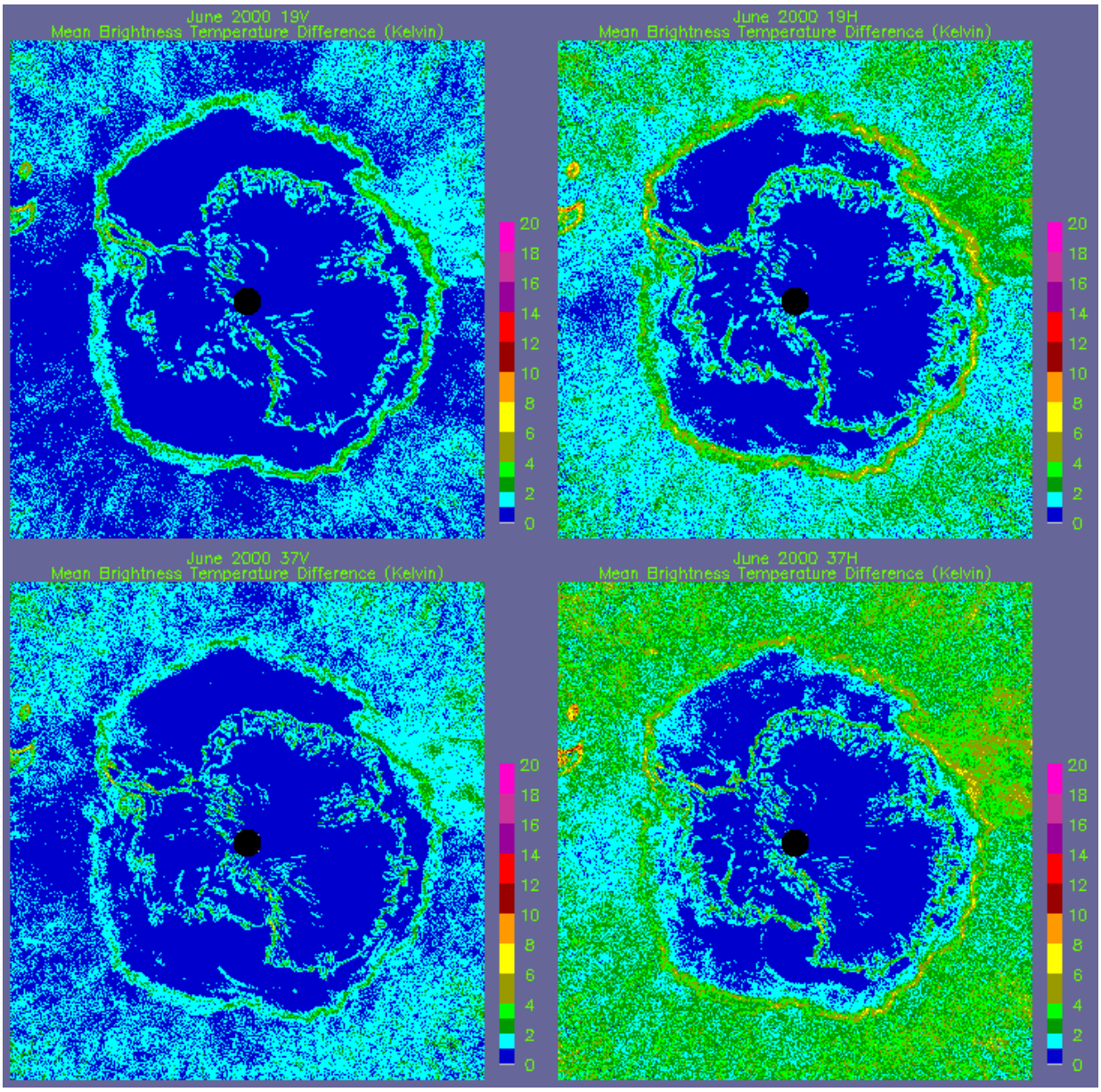

Figure 8. June 2000 Southern Hemisphere Tb Differences

Though there can be significant differences in the brightness temperatures at individual grid cells, the overall mean brightness temperatures for each grid are similar among products. For example, Tables 1 and 2 show the mean brightness temperatures and the standard deviations of the brightness temperature grids for 15 January 2000 and 15 June 2000, respectively. In addition, for all channels in both hemispheres, the ratio of the NRTSI product variances and the standard product falls between the tails of the F distribution at the 95% confidence level. Therefore, the hypothesis that the variances are equal, is valid.

Similarly, for the 19 GHz, 22 GHz, and 37 GHz channels in both hemispheres, the absolute value of the T statistic (the difference in the means divided by the "sample

standard deviation") is less than the Student's T distribution value for 0.025. Thus, the hypothesis that the means of the standard and NRTSI products are equal for these channels is valid. This hypothesis is not valid in all cases for the 85 GHz channels, because the T statistic exceeds the 95% confidence limit.

Table 1. Comparison of Gridded Brightness Temperatures for 15 January 2000

	Standard Products		NRTSI		Variance				
Channel	**Mean**	**Std. Dev.**	**Mean**	**Std. Dev.**	**Ratio**	**F(.975)**	**F(.025)**	**T Statistic**	**T(.025)**
19V North	224.45	28.11	224.45	28.11	1.0003	0.9891	1.0110	0.0106	1.9600
19H North	191.03	52.45	191.03	52.44	1.0004	0.9891	1.0110	0.0012	1.9600
22V North	227.24	21.47	227.21	21.46	1.0016	0.9891	1.0110	0.3146	1.9600
37V North	221.62	17.50	221.62	17.48	1.0021	0.9891	1.0110	0.0934	1.9600
37H North	193.90	34.83	193.89	34.81	1.0013	0.9891	1.0110	0.0579	1.9600
85V North	225.89	23.34	225.85	23.29	1.0039	0.9945	1.0055	0.7719	1.9600
85H North	207.63	21.93	207.58	21.88	1.0052	0.9945	1.0055	1.2827	1.9600
19V South	195.91	18.53	195.93	18.52	1.0007	0.9878	1.0123	0.3152	1.9600
19H South	138.81	33.65	138.82	33.64	1.0007	0.9878	1.0123	0.1093	1.9600
22V South	207.02	14.64	207.09	14.63	1.0008	0.9878	1.0123	1.0906	1.9600
37V South	212.20	10.96	212.24	10.96	0.9983	0.9878	1.0123	0.8104	1.9600
37H South	163.83	23.93	163.87	23.93	1.0000	0.9878	1.0123	0.3909	1.9600
85V South	236.51	15.67	236.65	15.65	1.0020	0.9939	1.0062	3.9346	1.9600
85H South	206.14	17.91	206.29	17.91	1.0000	0.9939	1.0062	3.6226	1.9600

Table 2. Comparison of Gridded Brightness Temperatures for 15 June 2000

	Standard Products		NRTSI		Variance				
Channel	**Mean**	**Std. Dev.**	**Mean**	**Std. Dev.**	**Ratio**	**F(.975)**	**F(.025)**	**T Statistic**	**T(.025)**
19V North	239.86	38.72	239.70	38.74	0.9987	0.9890	1.0111	1.0573	1.9600
19H North	207.36	64.77	207.10	64.82	0.9985	0.9890	1.0111	1.0349	1.9600
22V North	247.61	29.82	247.53	29.84	0.9990	0.9890	1.0111	0.6954	1.9600
37V North	245.95	28.24	245.87	28.24	0.9999	0.9890	1.0111	0.7260	1.9600
37H North	217.46	52.07	217.27	52.07	1.0000	0.9890	1.0111	0.9107	1.9600
85V North	259.90	16.68	260.06	16.65	1.0035	0.9945	1.0055	4.8769	1.9600
85H North	243.44	29.58	243.52	29.57	1.0002	0.9945	1.0055	1.4701	1.9600
19V South	204.84	27.37	204.82	27.36	1.0007	0.9876	1.0125	0.1254	1.9600
19H South	154.19	44.62	154.18	44.61	1.0005	0.9876	1.0125	0.0209	1.9600
22V South	211.27	23.29	211.20	23.27	1.0011	0.9876	1.0125	0.6298	1.9600
37V South	215.81	19.32	215.78	19.31	1.0016	0.9876	1.0125	0.3245	1.9600
37H South	174.17	31.67	174.15	31.64	1.0015	0.9876	1.0125	0.1480	1.9600
85V South	231.81	20.75	231.66	20.74	1.0015	0.9933	1.0068	3.2242	1.9600
85H South	204.92	22.11	204.76	22.08	1.0027	0.9933	1.0068	3.0999	1.9600

Although the corresponding products depict the same brightness temperature fields, substantial differences exist in the brightness temperatures at individual grid cells, particularly along coastlines. The most likely explanation for these differences is that RSS performs different geolocation calculations than GHRC. Figure 9 is a plot of the average distance between the nearest scans from each data set in 1-degree latitude belts for a single pass on 15 June 2000. Plots for other half orbits are similar. The average distance is about 13 km, or about half the footprint

size. A characteristic of the drop-in-the-bucket gridding algorithm is that each sample is assumed to be entirely within a single grid cell, and the value assigned to the grid cell is based entirely on the samples in the grid cell. The difference in geolocation of samples between the GHRC and RSS data sets means that samples are sometimes placed in different grid cells, which explains the difference in individual grid cell values. Therefore, geolocation differences become important along coastlines, sea ice boundaries, and ocean boundaries where differences in brightness temperatures between land, ocean, and sea ice are quite large. The larger differences observed over the open ocean may be a result of NSIDC's decision to not implement the adjustment for the differences between the antenna observations and Wentz' radiative transfer model in the standard product.

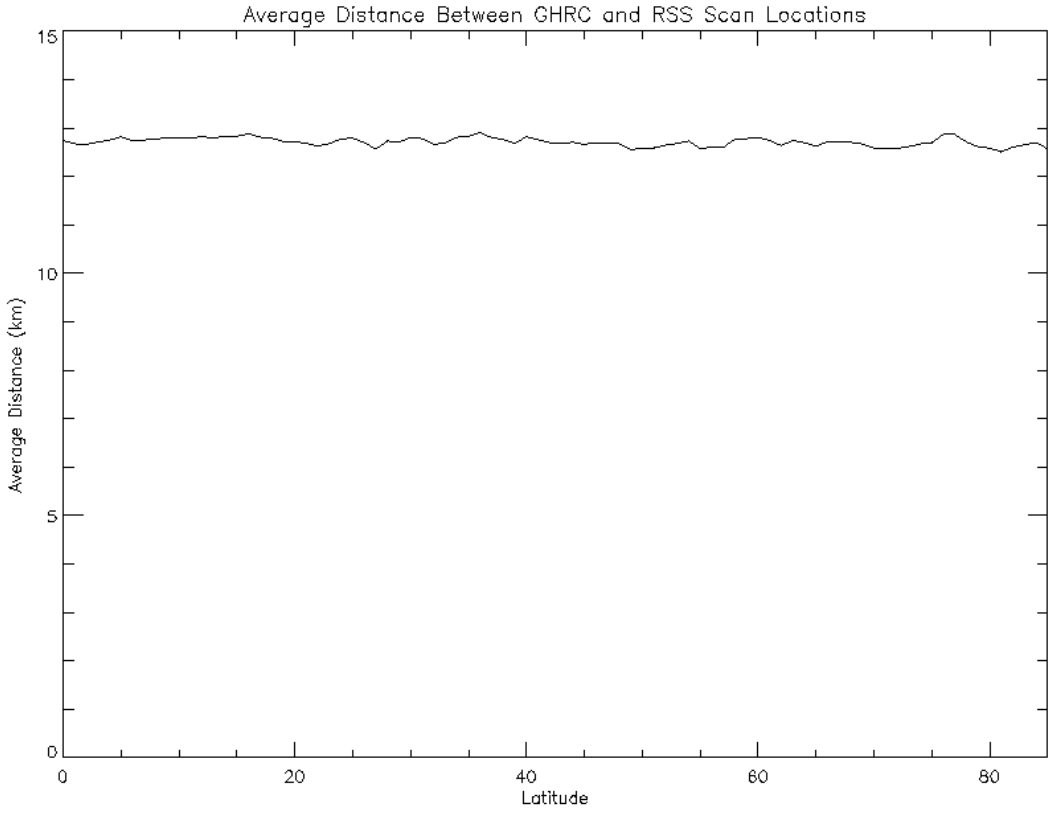

Figure 9. Difference Between GHRC and RSS Scan Locations

For approximately seven years, NSIDC did not apply the correction for the cold-space reflector interference problem to the RSS data. The bar graphs in Figures 10 and 11 compare the standard and NRTSI products for June 1999. Results are similar as those for the standard product that includes the along-scan correction (June 2000), but there are roughly 10% fewer grid cells that agree to within .1K.

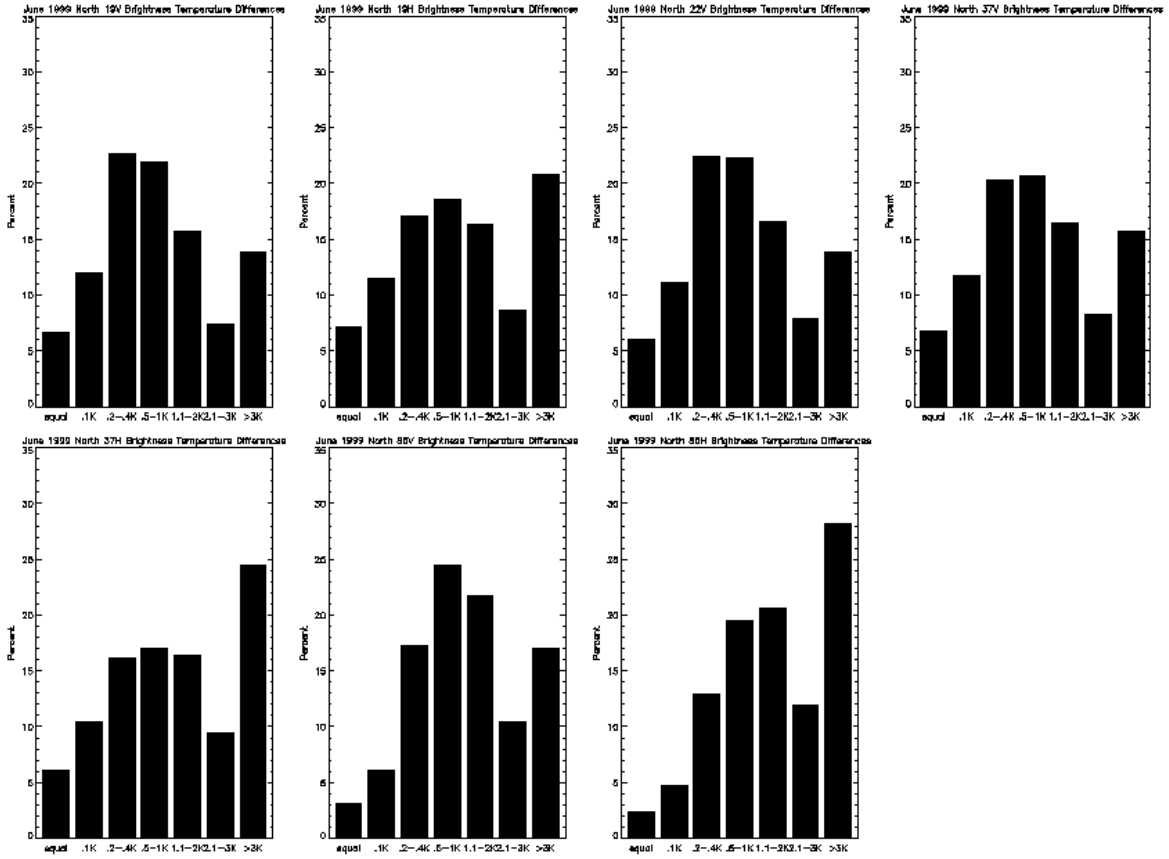

Figure 10. June 1999 Northern Hemisphere Brightness Temperature Difference Bar Graphs

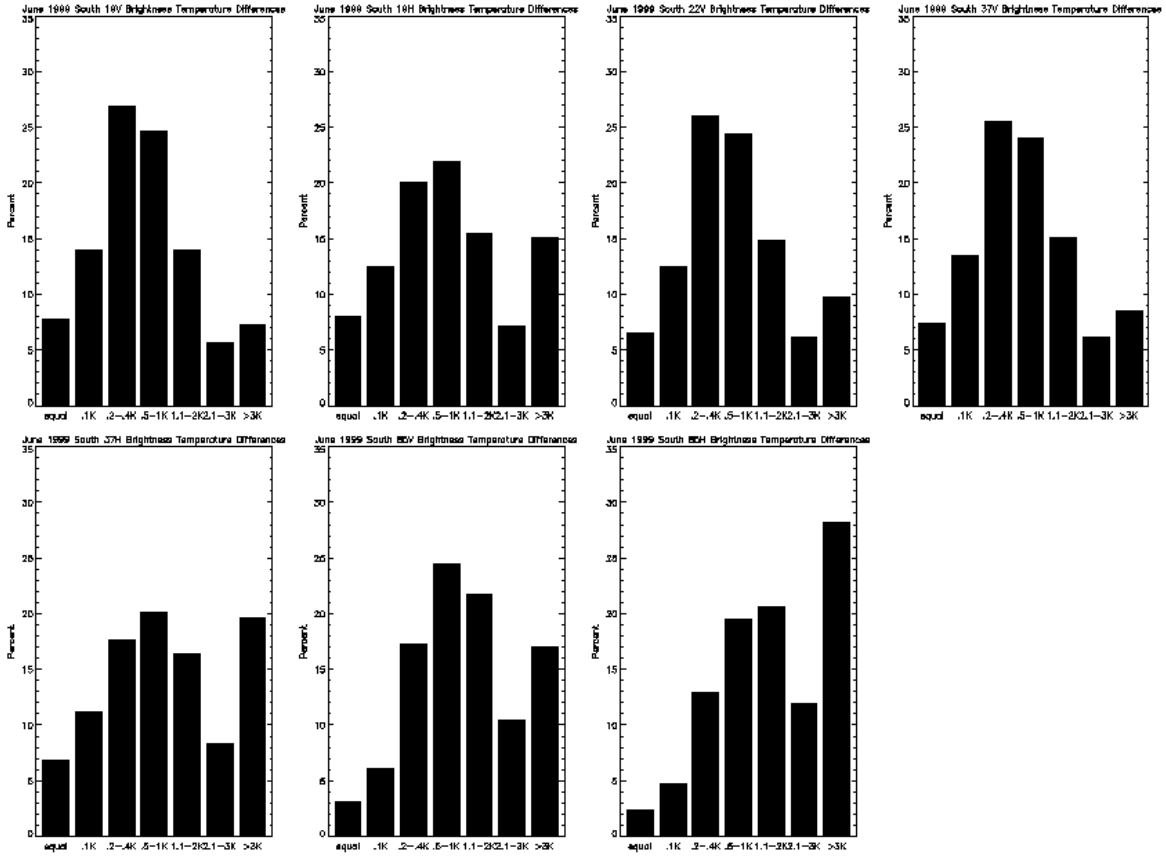

Figure 11. June 1999 Southern Hemisphere Brightness Temperature Difference Bar Graphs

Sea Ice Concentration Comparison

The differences in the brightness temperature grids do not translate into significant differences in the sea ice concentrations. As shown in Figure 12, the vast majority of the grid cells have identical sea ice concentrations. Virtually all agree to within 4%. Less than 1% of the grid cells differ by 5% or more.

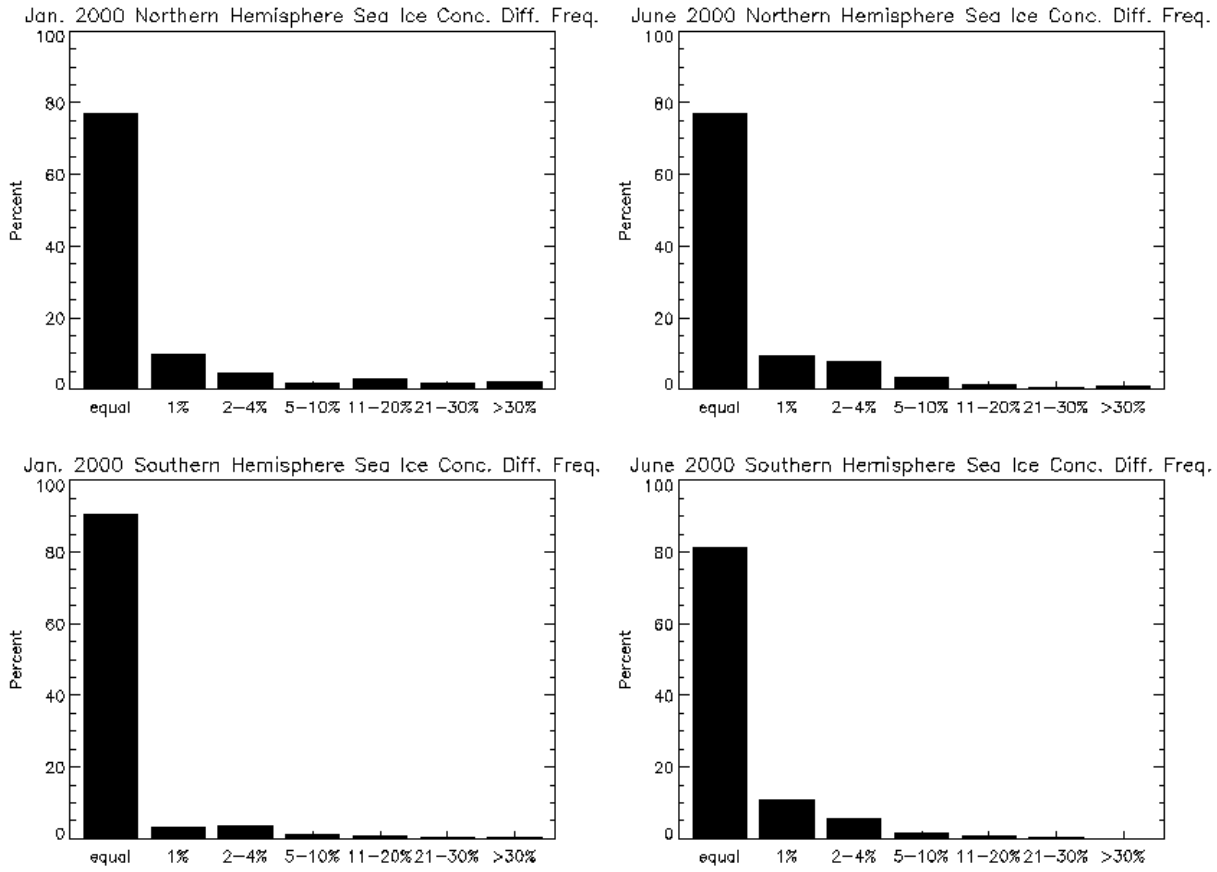

Figure 12. Sea Ice Difference Bar Graphs.

Figures 13 and 14 are analyses of where the sea ice concentration differences occur. Figure 13 shows the difference in sea ice concentration in each hemisphere on 15 January and 15 June 2000. The greatest differences occur along the coasts and at the ice margins. Some significant differences are also observed over the open ocean. Note that the large differences in the lower left in the Southern Hemisphere on 15 January show the effect of using a sea ice mask in the Near Real-Time DMSP SSM/I Daily Polar Gridded Sea Ice Concentration ice grids. The use of this mask has been discontinued (though it is still used in the Near Real-Time SSM/I EASE-Grid Daily Global Ice Concentration and Snow Extent).

Figure 14 shows the monthly mean differences for each grid cell during January and June 2000. The differences are negligible with the exception of a small area in the lower left region of the Southern Hemisphere in January. Again, this is due to the use of the sea ice mask. Sea ice concentration differences along the sea ice boundaries are greater than in the middle of the ice pack, but are still less than 10%.

The closer agreement of sea ice concentrations compared with brightness temperatures is not contradictory. Since all the brightness temperature channels are affected by the differences between the GHRC and RSS data sets in the same way, the brightness temperatures for each channel should generally differ in the same direction. Since the NASA Team sea ice algorithm uses brightness temperature ratios, effects of temperature variations are reduced.

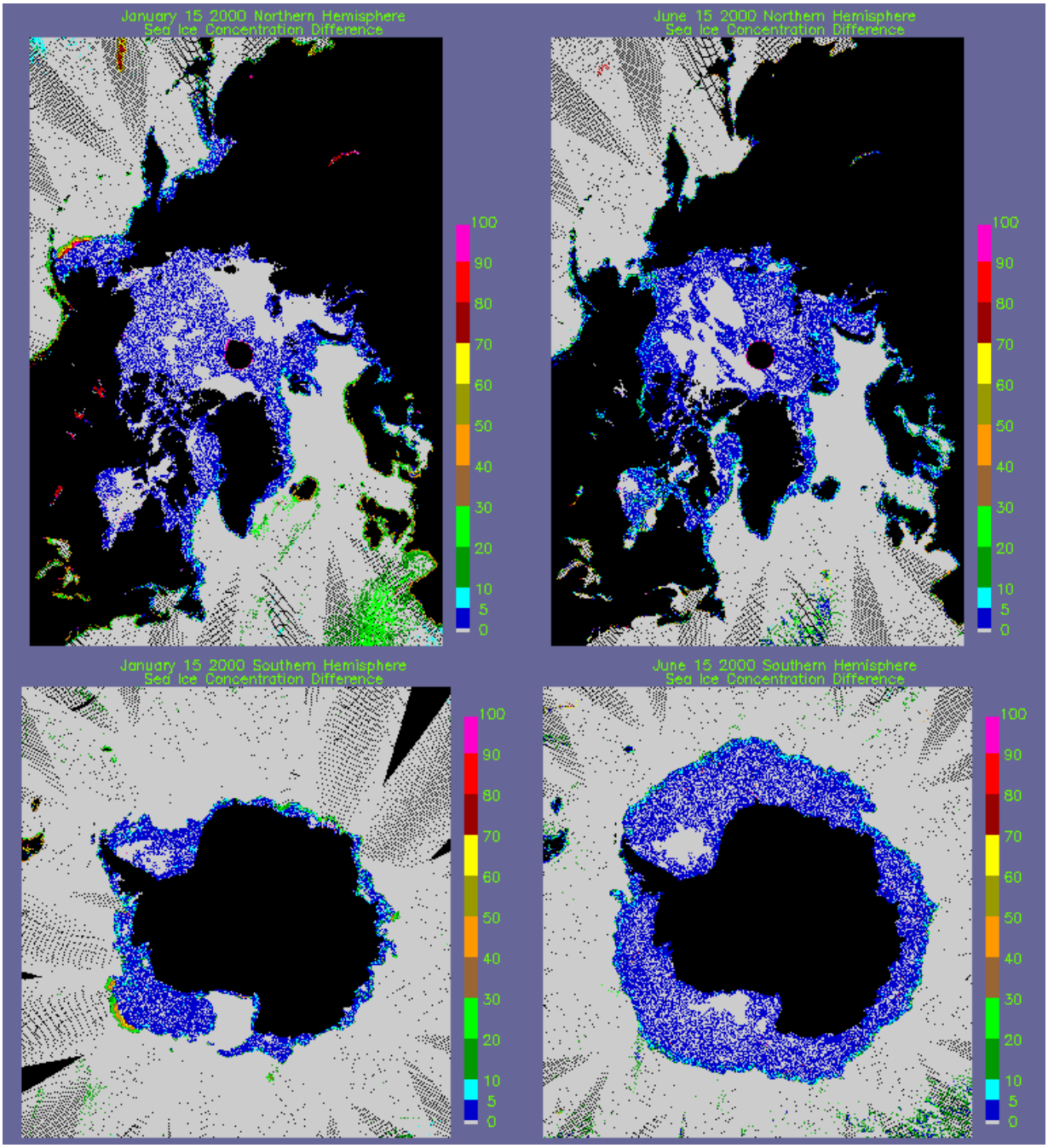

Figure 13. January 15 2000 and June 15 2000 Sea Ice Concentration Differences

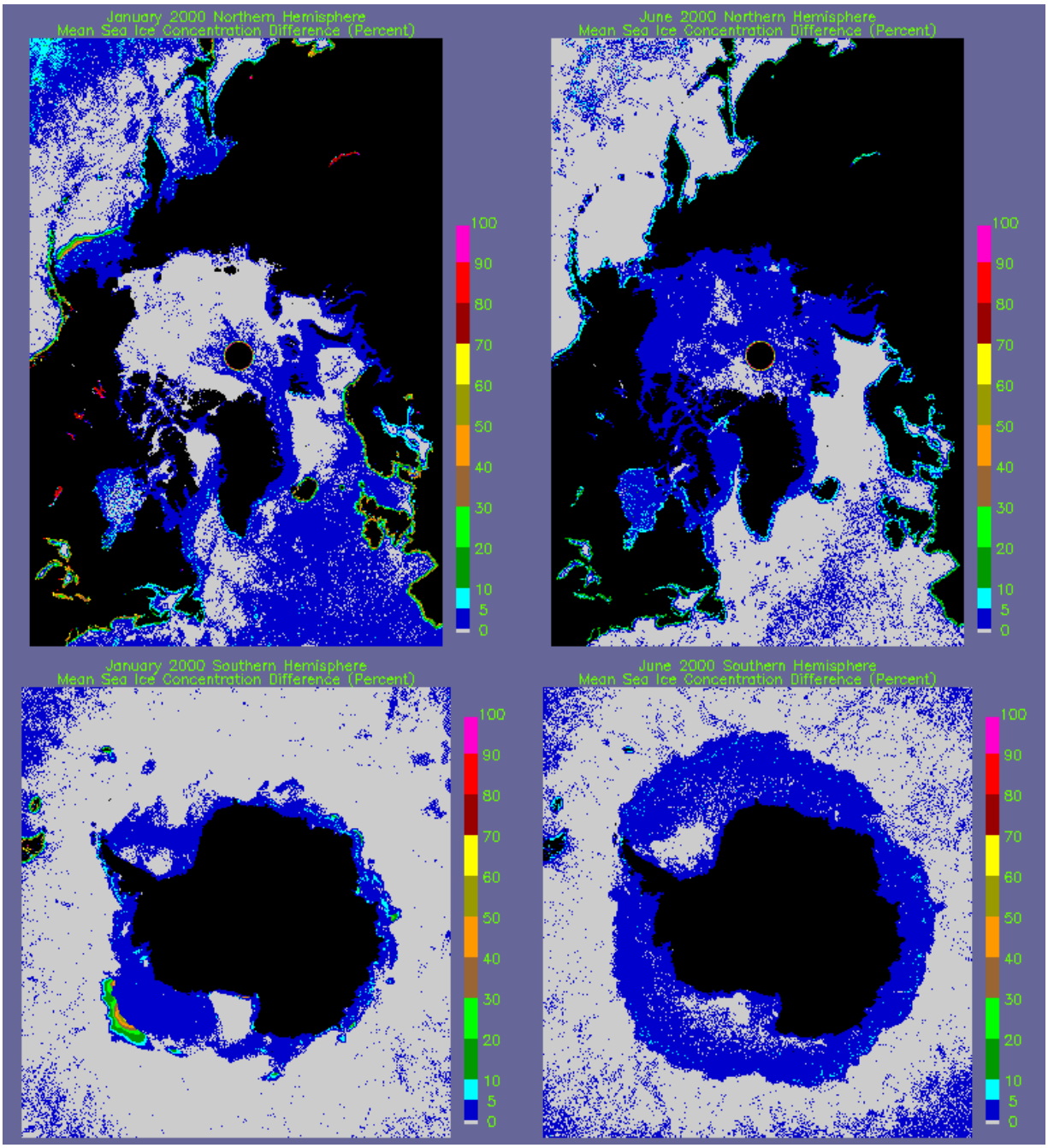

Figure 14. January 2000 and June 2000 Mean Sea Ice Concentration Differences

Summary and Conclusions

Near real-time brightness temperature and sea ice concentration products were compared with the standard NSIDC brightness temperature and sea ice products to gain a better understanding of their differences. The study concentrated on products created during the year 2000 when both product sets were generated from brightness temperature data that were corrected for cold-space reflector interference on the DMSP satellites. NSIDC also evaluated the effect of using

brightness temperatures that were not adjusted for the cold-space reflector problem.

NSIDC found noticeable differences between the brightness temperature products, but little difference between the sea ice concentration products. Since the greatest differences in the brightness temperatures were concentrated at coastlines and the boundaries of the sea ice, the differences were attributed to the use of different geolocation programs by the two different data suppliers.

NSIDC also found that not using the optional adjustment for the cold-space reflector interference slightly increased the difference between the two product sets.

References

Cavalieri, Don. 1996. NASA Team sea ice algorithm.

Knowles, K. 1993. Points, pixels, grids, and cells.

Stroeve, J. 1998. Impact of various processing options on SSM/I-derived brightness temperatures. NSIDC Special Report 7. Boulder, CO, USA: National Snow and Ice Data Center.

Wentz, Frank. 1992. *Final Report Production of SSM/I Data Sets.* RSS Technical Report 090192. Santa

Rosa, CA: Remote Sensing Systems.